Tracing the structure of asymmetric molecules from high-order harmonic generation

Yanjun Chen[1,*] and Bing Zhang[2,†]
[1]*Beijing Computational Science Research Center, Beijing, P. R. China*
[2]*Department of Physics, Harbin Institute of Technology, Harbin, P. R. China*
(Received 8 July 2011; published 3 November 2011)

We investigate high-order harmonic generation (HHG) from asymmetric molecules exposed to intense laser fields. We show that the emissions of odd and even harmonics depend differently on the orientation angle, the internuclear distance, as well as the effective charge. This difference mainly comes from different roles of intramolecular interference in the HHG of odd and even harmonics. These roles map the structure of the asymmetric molecule to the odd vs even HHG spectra.

DOI: 10.1103/PhysRevA.84.053402 PACS number(s): 32.80.Rm, 42.65.Ky

I. INTRODUCTION

In past years, high-order harmonic generation (HHG) from atoms and molecules in strong fields has attracted wide theoretical and experimental attention [1]. This interest in HHG arises from the important applications of HHG. For example, using HHG, one can obtain attosecond pulses, which are important for ultrafast time resolution. In addition, HHG also provides a new manner to probe the structure of matter [2].

Great progress has been made in the study of HHG both for theoretically and experimentally. HHG can be well understood by three-step models [3,4], where harmonics are emitted through the steps of tunneling, propagation, and recombination. In recent years, attention has been paid mainly to HHG from symmetric molecules, such as N_2 [2], H_2^+ [5], and CO_2 [6,7]. The multicenter characteristic of the molecular Coulomb potential is responsible for many interesting physical phenomena such as the alignment effect [2], the two-center interference effect [5], etc. For asymmetric molecules such as CO [8,9], HCl [10], and HeH^{2+} [11,12], interest in HHG is increasing. HHG is more complex in the latter cases. Due to symmetry breaking, some different effects appear, such as asymmetric ionization [11], enhanced excitation [12], etc. This asymmetry also induces the HHG of both odd and even harmonics. The mechanism for these two different HHG channels, to our knowledge, is not yet sufficiently well understood.

In this paper, we study HHG from asymmetric two-center model molecules with diverse effective charges and internuclear distances at different orientation angles. The numerical solution of the time-dependent Schrödinger equation (TDSE) shows that the emission of odd and even harmonics rely differently on the molecular parameters and angle. But the relative yields of odd vs even harmonics are characterized by these parameters and are not sensitive to the laser intensity. To explore the underlying physical mechanism, we use the continuum electronic wave packet generated from a symmetric molecule to recollide with the nuclei of the asymmetric molecule. This recollision produces HHG spectra that agree with the TDSE results. Using a model that we developed based on the simulations, we show that the two HHG channels of odd and even harmonics are subject to different interference effects. The effects arise from the two-center structure of the asymmetric Coulomb potential and influence significantly the HHG spectra of odd vs even harmonics. As a result, the property of the asymmetric potential can be traced from the odd vs even HHG spectra.

II. NUMERICAL SIMULATION

The Hamiltonian of two-center molecules studied here is

$$H(t) = \mathbf{p}^2/2 + V(\mathbf{r}) - \mathbf{r}\cdot\mathbf{E}(t)$$

(in atomic units of $\hbar = e = m_e = 1$). We use the soft-core Coulomb potential

$$V(x) = \frac{-Z_1}{\sqrt{0.5+(x+R_1)^2}} + \frac{-Z_2}{\sqrt{0.5+(x-R_2)^2}}$$

and

$$V(x,y) = \frac{-Z_1}{\sqrt{0.5+(x+R_1)^2+y^2}} + \frac{-Z_2}{\sqrt{0.5+(x-R_2)^2+y^2}}$$

for one-dimensional (1D) and two-dimensional (2D) cases. Here Z_1 and Z_2 are the effective charges, $R_1 = [Z_2/(Z_1+Z_2)]R$, and $R_2 = [Z_1/(Z_1+Z_2)]R$. R is the internuclear separation. $\mathbf{E}(t) = \vec{\mathbf{e}}_\theta E \sin\omega_0 t$ is the external electric field with the amplitude E and the frequency ω_0. $\vec{\mathbf{e}}_\theta$ is the unit vector along the laser polarization and θ is the angle between the molecular axis and the laser polarization. We use trapezoidally shaped laser pulses with a total duration of 10 optical cycles and linear ramps of three optical cycles in the calculations. The details for the numerical solution of the TDSE are introduced in Ref. [13]. The HHG spectrum is obtained by [5]

$$F(\omega,\theta) = \int \langle\psi(t)|\vec{\mathbf{e}}_\theta\cdot\nabla V|\psi(t)\rangle e^{i\omega t}dt, \qquad (1)$$

where $|\psi(t)\rangle$ is the time-dependent wave function of $H(t)$ and ω is the emitted-proton frequency. Omitting the contribution of the continuum-continuum (c-c) transition [4], Eq. (1) can be approximated as [14] $F(\omega,\theta) \approx \sum_n \int \langle n|\vec{\mathbf{e}}_\theta\cdot\nabla V|\psi(t)\rangle a_n^*(t)e^{i\omega t}dt$. Here, $|n\rangle$ is the bound state of the field-free Hamiltonian $H_0 = \mathbf{p}^2/2 + V(\mathbf{r})$ and $a_n(t) = \langle n|\psi(t)\rangle$. For cases in this paper, our calculations show that the main contribution to harmonics comes from the initial state $|0\rangle$ (the ground state of H_0). We have $F(\omega,\theta) \approx F_0(\omega,\theta)$ with

*chenyjhb@gmail.com
†Bingzhanghit@yahoo.cn

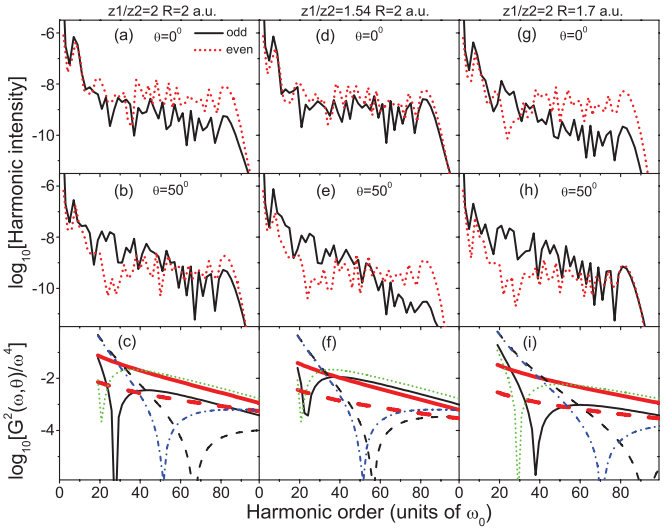

FIG. 1. (Color online) Harmonic spectra of 2D asymmetric molecules with the same ionization potential $I_p = 1.1$ a.u. but diverse effective charges Z_1 and Z_2 and internuclear distances R at $\theta = 0^\circ$ [(a), (d), and (g)] and $\theta = 50^\circ$ [(b), (e), and (h)] for odd (solid black curves) and even (dotted red curves) harmonics, obtained using Eq. (1) with $I = 5 \times 10^{14}$ W/cm^2 and $\lambda = 780$ nm. Results in each column are obtained for the same molecular parameters shown at the top of the column. In panels (c), (f), and (i), we also show the corresponding interference factors $|G_{\rm odd}(\omega,\theta)|^2/\omega^4$ of Eq. (3) at $\theta = 0^\circ$ (thin black solid curves) and at $\theta = 50^\circ$ (thin black dashed curves), and $|G_{\rm even}(\omega,\theta)|^2/\omega^4$ of Eq. (4) at $\theta = 0^\circ$ (bold red solid curves) and at $\theta = 50^\circ$ (bold red dashed curves). There, we also show the interference factor $|G^{\rm sy}_{\rm odd}(\omega,\theta)|^2/\omega^4$ of H_2^+ with the same internuclear distance R as the corresponding asymmetric molecule at $\theta = 0^\circ$ (dotted green curves) and at $\theta = 50^\circ$ (dot-dashed blue curves).

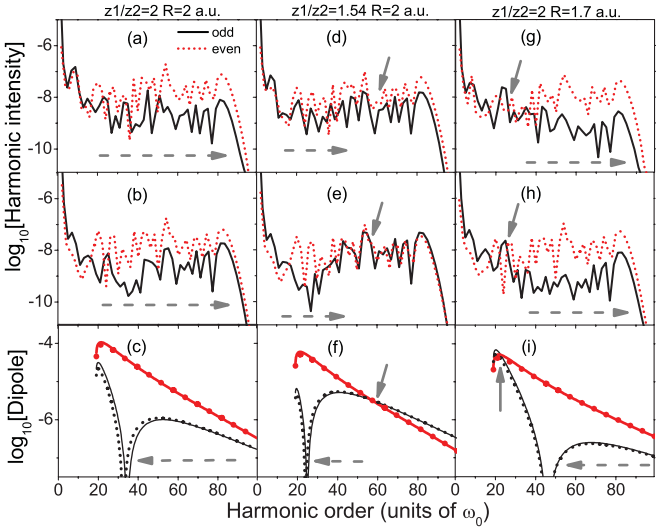

FIG. 2. (Color online) Harmonic spectra of 1D asymmetric molecules with the same ionization potential $I_p = 1.1$ a.u. but diverse effective charges Z_1 and Z_2 and internuclear distances R for odd (solid black curves) and even (dotted red curves) harmonics, obtained using Eq. (1) [(a), (d), and (g)] and Eq. (2) [(b), (e), and (h)] with $I = 5 \times 10^{14}$ W/cm^2 and $\lambda = 780$ nm. Results in each column are obtained for the same molecular parameters shown at the top of the column. In panels (c), (f), and (i), we also show the relevant dipoles $|\langle 0|\nabla V|\mathbf{p}\rangle|^2/\omega^4$ of the model molecules with the continuum energy $E_{\mathbf{p}} = \omega - I_p$. Here, the solid curves show the exact results with $|\mathbf{p}\rangle$ being the odd-like-parity (thin black solid curves) or even-like-parity (bold red solid curves) continuum eigenstates of the asymmetric molecules. The dotted curves show the simulated ones with $|\mathbf{p}\rangle$ being the odd-parity (thin black dotted curves) or even-parity (bold red dotted curves) continuum eigenstate of H_2^+. The dashed arrows indicate the interference-induced hollows in dipoles or spectra. The solid arrows indicate the intersections of the odd vs even spectra or the odd- vs even-parity-part dipoles.

$F_0(\omega,\theta) = \int \langle 0|\vec{\mathbf{e}}_\theta \cdot \nabla V|\psi(t)\rangle a_0^*(t) e^{i\omega t} dt$. To identify the role of the asymmetric Coulomb potential in HHG, we first solve the TDSE of a symmetric molecule with a similar ionization potential as the asymmetric molecule under consideration. In each time step in $F_0(\omega,\theta)$, we replace $|0\rangle$ and $V(\mathbf{r})$ of the symmetric molecule by $|0_{\rm as}\rangle$ and $V_{\rm as}(\mathbf{r})$ of the asymmetric model. We have

$$F_0'(\omega,\theta) = \int \langle 0_{\rm as}|\vec{\mathbf{e}}_\theta \cdot \nabla V_{\rm as}|\psi(t)\rangle a_0^*(t) e^{i\omega t} dt. \qquad (2)$$

Equation (2) denotes a simulated recollision between the continuum electronic wave packet of a symmetric molecule and the nuclei of an asymmetric molecule. We have simulated the HHG of asymmetric molecules using Eqs. (1) and (2). Results are presented in Figs. 1–3. For comparison, the initial states of the molecules studied have the same ionization potential $I_p = 1.1$ a.u. in Figs. 1 and 2 and $I_p = 2.25$ a.u. in Fig. 3. In addition, in the use of Eq. (2) in this paper, a symmetric molecule with $R = 2$ a.u. (H_2^+) has been chosen to generate the continuum wave packet for cases of $I_p = 1.1$ a.u. and another with $R = 4$ a.u. for cases of $I_p = 2.25$ a.u. As we will show in the following, the HHG spectra of the asymmetric molecules with similar I_p are characterized by the molecular parameters of Z_1/Z_2 and R.

In the first two rows of Fig. 1, we plot the characteristic HHG spectra of 2D asymmetric molecules with diverse molecular parameters at different angles. In our simulations, odd and even harmonics are well resolved. For clarity, we link them using solid or dotted lines. First, the HHG spectra in Fig. 1 show that the yields of even harmonics decrease significantly as the angle increases. However, a careful comparison shows that, for all cases presented here, the even-order HHG spectra in the plateau are similar with each other within a vertical scaling factor. Second, the odd-order HHG spectra differ remarkably for different angles and molecular parameters. But as the parameters change, the yields of some harmonics increase and others diminish. As a result, the relative yields of odd vs even harmonics in each subpanel are characterized by the corresponding parameters. For example, in Fig. 1(a), the yields of odd harmonics are one order of magnitude lower than those of the even harmonics in the plateau. Those are comparable in Fig. 1(d). In Fig. 1(g), the dotted red curve is higher than the solid black curve for low orders. The situation reverses for high orders. This reverse, which is related to a well-defined intersection of these two curves, occurs at the 30th order. This intersection is not observed in Figs. 1(a) and 1(d). Below, the term "intersection" is used to direct to this reverse. These different behaviors of odd and even harmonics have been checked in other three-dimensional simulations. Particularly, as the laser intensity increases, except for the cutoff position,

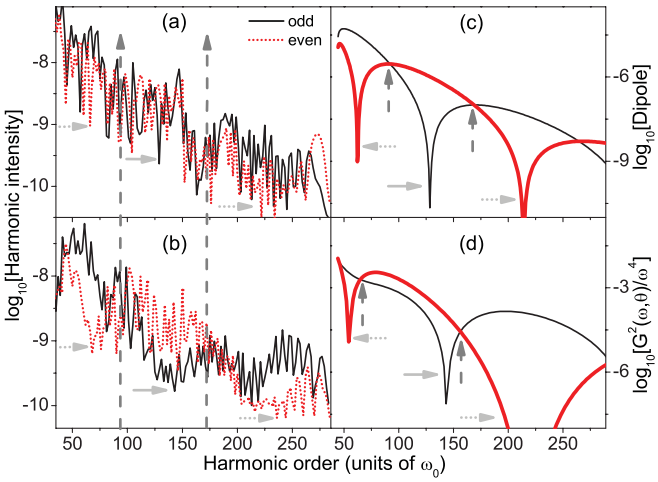

FIG. 3. (Color online) Harmonic spectra of 2D HeH^{2+} with $I_p = 2.25$ a.u., $Z_1/Z_2 = 2$, and $R = 4$ a.u. for odd (solid black curves) and even (dotted red curves) harmonics, obtained using Eq. (1) [shown in (a)] and Eq. (2) [shown in (b)] with $I = 1.2 \times 10^{15}$ W/cm^2 and $\lambda = 900$ nm at $\theta = 0^\circ$. Results in (c) show the 1D exact dipole $|\langle 0|\nabla V|\mathbf{p}\rangle|^2/\omega^4$ of HeH^{2+} with the continuum energy $E_\mathbf{p} = \omega - I_p$ for $|\mathbf{p}\rangle$ having the odd-like (thin black curve) or even-like (bold red curve) parity. Results in (d) show the interference factors $|G_{\rm odd}(\omega,\theta)|^2/\omega^4$ of Eq. (3) (thin black curve) and $|G_{\rm even}(\omega,\theta)|^2/\omega^4$ of Eq. (4) (bold red curve) of this asymmetric molecule at $\theta = 0^\circ$. The horizontal solid (dotted) arrows indicate the interference minima in the odd-parity-part (even-parity-part) dipole, the interference factor of $G_{\rm odd}$ ($G_{\rm even}$), or the odd-order (even-order) spectrum. The vertical dashed arrows indicate the intersections of the odd- vs even-parity-part dipoles, the interference factors of $G_{\rm odd}$ vs $G_{\rm even}$, or the odd vs even spectra.

the main characteristics of the odd vs even spectra hold in other calculations. Since results are similar, we do not show them here. To understand Fig. 1, Eq. (2) is used. For the 2D cases in Fig. 1, Eq. (2) produces HHG spectra very similar to those presented here for both odd and even harmonics. This implies that the continuum wave packets generated from the asymmetric molecules are similar to the symmetric ones here. It can then be concluded that the recombination step is mainly responsible for the phenomena shown above. To clarify this conclusion, we turn in the following to 1D cases, where a full-quantum analysis of HHG can be performed [14]. We will return to Fig. 1 later.

In Fig. 2, we plot 1D spectra of asymmetric molecules with the molecular parameters similar to the 2D parameters used in Fig. 1. The corresponding results in the first two rows of Fig. 2 obtained using Eqs. (1) and (2) are similar. They are also comparable with the relevant 2D results at $\theta = 0^\circ$ in Fig. 1. To achieve a full-quantum analysis of HHG, we project $|\psi(t)\rangle$ onto the eigenstates of H_0 of the system and only consider the continuum-bound transition [14]. Then the expression of $F_0(\omega,\theta)$ can be written as $F_0(\omega,\theta) \approx \int d\mathbf{p}[a(\mathbf{p},\omega)\langle 0|\vec{\mathbf{e}}_\theta \cdot \nabla V|\mathbf{p}\rangle]$. $a(\mathbf{p},\omega) = \int dt[a_0^*(t)c_\mathbf{p}(t)e^{i\omega t}]$ is the spectral amplitude. $\langle 0|\nabla V|\mathbf{p}\rangle$ is the dipole moment between the continuum eigenstate $|\mathbf{p}\rangle$ and the bound eigenstate $|0\rangle$ of H_0 of the asymmetric molecule. Similarly, Eq. (2) of $F_0'(\omega,\theta)$ can be written as $F_0'(\omega,\theta) \approx \int d\mathbf{p}[a(\mathbf{p},\omega)\langle 0_{\rm as}|\vec{\mathbf{e}}_\theta \cdot \nabla V_{\rm as}|\mathbf{p}\rangle]$. $\langle 0_{\rm as}|\nabla V_{\rm as}|\mathbf{p}\rangle$ is the simulated dipole of the asymmetric molecule. Note, here, that $|\mathbf{p}\rangle$ is the continuum eigenstate of the symmetric molecule H_2^+. We have calculated the exact and the simulated dipoles for the 1D asymmetric molecules. Results are shown in the last row of Fig. 2. One can see that the curves obtained using different methods agree well with each other. The simulated dipole in each subpanel can be divided into two parts; that is, the thin black dotted and the bold red dotted parts, which correspond to the odd-parity and even-parity states $|\mathbf{p}\rangle$ of H_2^+, respectively. For the simulated spectra in the second row of Fig. 2, our analysis shows that the main contribution to odd or even harmonics comes from $|\mathbf{p}\rangle$ having the odd or even parity, respectively. For the TDSE spectra in the first row of Fig. 2, the situation is similar. Our analysis shows that the continuum eigenstates $|\mathbf{p}\rangle$ of the asymmetric molecules studied here have the odd-like or even-like "parity." According to this "parity" of $|\mathbf{p}\rangle$, the exact dipoles $\langle 0|\nabla V|\mathbf{p}\rangle$ of the asymmetric molecules in Fig. 2 can also be divided into the odd-parity (thin black solid curves) and even-parity (bold red solid curves) parts. The main contribution to odd or even TDSE harmonics also comes from $|\mathbf{p}\rangle$ having the odd-like or even-like "parity." Thus, the odd or even HHG spectrum of the asymmetric molecule is related to the odd-parity-part or even-parity-part dipole of the molecule.

Further comparisons show that the relevant spectra and dipoles in each column of Fig. 2 behave similarly. For example, the thin black solid curve of the odd-parity-part dipole in Fig. 2(c) shows a broad interference-induced hollow [14] around the 33rd order, as indicated by the dashed arrow. The odd harmonics are suppressed in the whole plateau in Fig. 2(a). The curves in Fig. 2(i) show an intersection located at the 23rd order, as indicated by the solid arrow. The spectra in Fig. 2(g) intersect at the 26th order. These results imply that the structure of the asymmetric molecule is mapped directly in the HHG spectrum. In fact, if we assume that the main contribution to one harmonic ω comes from electrons with energy $E_\mathbf{p} = \omega - I_p$ [2], we have $F_0(\omega,\theta) \approx a(\mathbf{p},\theta)\langle 0|\vec{\mathbf{e}}_\theta \cdot \nabla V|\mathbf{p}\rangle$. The expression shows the close relation between dipoles and spectra. Note that, in the above expression, the emission of odd or even harmonics from asymmetric molecules is related to the continuum eigenstate $|\mathbf{p}\rangle$ having the odd-like or even-like "parity." In particular, the similarity between the exact results and the simulated ones for the dipoles and the spectra in Fig. 2 also tells that (1) the continuum eigenstate $|\mathbf{p}\rangle$ of the asymmetric molecule in the expression can be approximated by the symmetric one; (2) for the present cases, the spectral amplitude $a(\mathbf{p},\theta)$ in the expression is not sensitive to the molecular parameters. These suggest that the structure of the asymmetric molecule can also be traced from the HHG spectra using the molecular orbital tomography procedure [2].

III. ANALYTICAL EXPRESSION

With these analyses, we now explore the analytical expression for the part of the dipole, which is mainly responsible for the emission of odd or even harmonics. We assume that the ground-state wave function of the asymmetric molecule is $\phi_0(\mathbf{r}) = \langle \mathbf{r}|0\rangle = P(a_1 e^{-\kappa r_a} + a_2 e^{-\kappa r_b})$ with $a_1 = Z_1/B$, $a_2 = Z_2/B$, $B = (Z_1^2 + Z_2^2)^{1/2}$, $r_a = |\mathbf{r} + R_1|$, $r_b = |\mathbf{r} - R_2|$, and $\kappa = \sqrt{2I_p}$. P is the normalization factor. The dipole along the laser polarization can be written as $\langle 0|\vec{\mathbf{e}}_\theta \cdot \mathbf{r}|\mathbf{p}\rangle$. Here, $|\mathbf{p}\rangle \propto e^{i\mathbf{p}_k\cdot\mathbf{r}}$ is the plane wave with energy $E_\mathbf{p}$. $\mathbf{p}_k$ is the effective

momentum with $p_k = |\mathbf{p}_k| = [2(I_p + E_\mathbf{p})]^{1/2}$ that considers the Coulomb effect [13]. The part of the dipole relating to the odd-parity component of $|\mathbf{p}\rangle$ is $D_{\rm odd}(\omega,\theta) = \int d\mathbf{r}[\phi_0(\mathbf{r})\vec{\mathbf{e}}_\theta \cdot \mathbf{r}\sin(\mathbf{p}_k \cdot \mathbf{r})]$ with $\omega = E_\mathbf{p} + I_p$. $D_{\rm odd}(\omega,\theta)$ is mainly responsible for the emission of odd harmonics, as discussed above. We assume that $|\mathbf{p}\rangle$ is orthogonal to $e^{-\kappa r}$ and consider the momenta $\mathbf{p}$ parallel to $\vec{\mathbf{e}}_\theta$, which contribute importantly to HHG [4]. We have $D_{\rm odd}(\omega,\theta) \propto G_{\rm odd}(\omega,\theta)\int d\mathbf{r}[e^{-\kappa r}\vec{\mathbf{e}}_\theta \cdot \mathbf{r}\sin(\mathbf{p}_k \cdot \mathbf{r})]$ with

$$G_{\rm odd}(\omega,\theta) = a_1\cos(p_k R_1\cos\theta) + a_2\cos(p_k R_2\cos\theta). \quad (3)$$

$G_{\rm odd}(\omega,\theta)$ is the interference factor in the dipole for the emission of odd harmonics. Similarly, the interference factor for the emission of even harmonics is

$$G_{\rm even}(\omega,\theta) = a_1\sin(p_k R_1\cos\theta) - a_2\sin(p_k R_2\cos\theta). \quad (4)$$

These two above expressions are the main conclusion of this paper. They reveal the important role of intramolecular interference in the HHG of asymmetric molecules. They show that the two HHG channels of odd and even harmonics are subject to different interference effects of cos and sin. These interference effects rely on all the molecular parameters and the angle. For symmetric molecules such as H_2^+, we have $G^{\rm sy}_{\rm even}(\omega,\theta) = 0$ and $G^{\rm sy}_{\rm odd}(\omega,\theta) \sim \cos[p_k(R/2)\cos\theta]$. One returns to the familiar cos interference pattern in the HHG of H_2^+ [5]. For $\theta = 90^\circ$, $G_{\rm even}(\omega,\theta) \equiv 0$ and $G_{\rm odd}(\omega,\theta) \equiv$ const. This implies that the interference effect disappears and the molecule behaves similarly to a single atom. The applicability of the expressions is shown in the last row of Fig. 1. There, we plot the function curves of $|G_{\rm odd}(\omega,\theta)|^2$ (thin black curves) and $|G_{\rm even}(\omega,\theta)|^2$ (bold red curves) at $\theta = 0^\circ$ (solid curves) and $\theta = 50^\circ$ (dashed curves) for the relevant molecular parameters in each column. For comparison, we also show the curves of $|G^{\rm sy}_{\rm odd}(\omega,\theta)|^2$ of H_2^+ at $\theta = 0^\circ$ (dotted green curves) and $\theta = 50^\circ$ (dot-dashed blue curves). The curves are divided by a factor ω^4 to compare with the spectra. It can be seen here that the curves of $G_{\rm odd}$ show a minimum located at different orders for different parameters. The curves of $G_{\rm even}$ are similar within a vertical scaling factor for different parameters. These explain the different behaviors of odd and even harmonics observed in the first two rows of Fig. 1. In particular, the curves of $G_{\rm odd}(\omega,\theta)$ and $G_{\rm even}(\omega,\theta)$ also predict the relative yields of odd vs even harmonics. For example, the odd and even spectra in Fig. 1(b) of $\theta = 50^\circ$ show an intersection at the 53rd order. This is near to the 46th order predicted by the dashed curves in Fig. 1(c). In Fig. 1(d) of $\theta = 0^\circ$, the odd and even spectra are near to each other. This is also seen in Fig. 1(f) for the solid curves. It should be noted that the interference patterns of asymmetric molecules differ from the symmetric ones remarkably. For example, in Fig. 1(c), the position of the minimum in the dot-dashed blue curve is at the 51st order. It is at the 67th order in the thin black dashed curve there. This remarkable difference has been shown in Ref. [9] for CO. We stress that the HHG of even harmonics from asymmetric molecules is also subject to the sine-type interference effect, as revealed by Eq. (4). For the present cases with small R, this sine interference pattern is not striking. For larger R, the situation changes, as shown in Fig. 3.

Figure 3(a) plots the HHG spectra of 2D HeH^{2+} with $R = 4$ a.u. at $\theta = 0^\circ$. The spectra of odd and even harmonics in Fig. 3(a) can be divided into three parts, as indicated by the dashed arrows. For low orders, the yields of the odd harmonics are higher than the even harmonics, and a minimum at the 66th order in the even spectrum, as indicated by the first dotted arrow, can be seen. For intermediate orders, which are near the cutoff (about the 150th order) of the first plateau [11], the odd and even HHG spectra are strongly oscillating. This oscillation is believed to arise from asymmetry ionization [12] and complicates the structure of the spectra. However, a careful comparison shows that around the 129th order in the first plateau, as indicated by the solid arrow, the yields of the even harmonics are one order of magnitude higher than the odd ones. For high orders, the situation is similar to that for low orders and a minimum at the 222nd order in the even spectrum, as indicated by the second dotted arrow, can be identified clearly. These behaviors agree with the predictions of the 1D exact dipole of HeH^{2+} with $R = 4$ a.u. in Fig. 3(c) and that of Eqs. (3) and (4) in Fig. 3(d), all for the minima in the odd or even HHG spectra (indicated by the solid or dotted arrows) and for the intersections of these spectra (indicated by the dashed arrows).

The TDSE spectra in Fig. 3(a) are also comparable with the simulated ones obtained using Eq. (2) in Fig. 3(b), especially for low and high orders. We stress that, in Fig. 3(b), the continuum wave packet is generated from a symmetric molecule and the asymmetric ionization does not occur. In fact, the behaviors of the simulated spectra in Fig. 3(b) match well with the relevant curves of the 1D exact dipole in Fig. 3(c), all for the minima and the intersections, as indicated by the corresponding arrows. This implies that, without the asymmetric ionization, the spectra and dipoles of asymmetric molecules with larger R can also show the close relation as in previous cases of small R. Particularly, our further simulations show that using higher laser intensities and longer wavelengths will further improve the agreement between the TDSE spectra and the simulated spectra using Eq. (2). This suggests that the influence of asymmetric ionization on HHG can diminish as the laser intensity and wavelength increase. These above analyses give suggestions on orbital tomography experiments [2] of asymmetry molecules with larger R using HHG.

Before conclusion, we append that (1) the theoretical predictions of Eqs. (3) and (4) in Fig. 3(d) match the exact results in Fig. 3(c) on the whole. But there is still a quantitative difference between them, both for the positions of the minima and the intersections of the curves. This difference is also seen between the 1D exact dipoles in Fig. 2 and those corresponding theoretical curves of Eqs. (3) and (4) for $\theta = 0^\circ$ in Fig. 1. For example, compared to Fig. 3(c), the minimum in the thin black curve in Fig. 3(d) appears at a higher order. This difference is expected to mainly arise from the plane-wave approximation that omits the Coulomb effect on the continuum electron. The use of the effect momentum p_k that partly considers the Coulomb effect in our analyses diminishes this difference to some extent. A better description of the Coulomb effect on the continuum electron is directed to the two-center Coulomb continuum wave function [15]. (2) The interference minimum we discuss in this paper is related to the odd or the even HHG spectrum. Around this minimum, the yields of odd and even harmonics usually differ

significantly, as suggested by Eqs. (3) and (4). This difference will help to identify the minimum in experiments. Besides the minimum, the intersection of the odd and the even HHG spectra should also be paid attention to. It gives other insights into the structural properties of the asymmetric molecule. In some cases, compared to the interference minimum, this intersection can be more easily identified in experiments. (3) The asymmetric molecule has a permanent dipole due to the asymmetry of the nuclei. This permanent dipole induces asymmetric ionization of the molecule in external fields. For asymmetric molecules with small internuclear distances R, the ionization of the asymmetric molecule is atomic-like [16]. This suggests that the influence of asymmetric ionization on the HHG is small. As shown in Fig. 2, the spectra for molecules with small R obtained using Eqs. (1) and (2) are similar. The permanent dipole of the asymmetric molecule is not included in the simulations using Eq. (2). For asymmetric molecules with intermediate R, asymmetric ionization can play an important role in HHG [16]. One important mechanism contributing to asymmetric ionization for intermediate R is that the excitation of the electron is enhanced by near-resonance tunneling when the direction of the laser field is antiparallel to the permanent dipole. This enhanced excitation results in multichannel HHG and fractional-order harmonics [12]. The use of the long laser wavelength in our simulations diminishes the excitation to some extent. In this situation, the main characteristics of the TDSE HHG spectra of odd vs even harmonics still match the predictions of the corresponding dipoles, as discussed in Fig. 3.

IV. CONCLUSION

In summary, we have studied HHG from asymmetric molecules. We show that intramolecular interference plays different roles in the emission of odd and even harmonics. As a result, the spectra of odd and even harmonics show different modulations that rely on all the molecular and laser parameters, such as the effective charge, the internuclear separation, and the orientation angle. The different interference effects for the HHG of odd and even harmonics arise from the property of the asymmetric Coulomb potential and are expected to appear in many other asymmetric molecules. We show the close relation between the odd vs even HHG spectra and the relevant dipoles. The relation gives suggestions on imaging the structure of the asymmetric molecule using HHG.

ACKNOWLEDGMENTS

This work is supported by the CAEP Foundation Project No. 2011B0102031.

[1] H. J. Wörner, J. B. Bertrand, D. V. Kartashov, P. B. Corkum, and D. M. Villeneuve, Nature (London) **466**, 604 (2010).
[2] J. Itatani, J. Levesque, D. Zeidler, Hiromichi Niikura, H. Pepin, J. C. Kieffer, P. B. Corkum, and D. M. Villeneuve, Nature (London) **432**, 867 (2004).
[3] P. B. Corkum, Phys. Rev. Lett. **71**, 1994 (1993).
[4] M. Lewenstein, Ph. Balcou, M. Yu. Ivanov, Anne L'Huillier, and P. B. Corkum, Phys. Rev. A **49**, 2117 (1994).
[5] M. Lein, N. Hay, R. Velotta, J. P. Marangos, and P. L. Knight, Phys. Rev. Lett. **88**, 183903 (2002).
[6] T. Kanai, S. Minemoto, and H. Sakai, Nature (London) **435**, 470 (2005).
[7] C. Vozzi *et al.*, Phys. Rev. Lett. **95**, 153902 (2005).
[8] S. De *et al.*, Phys. Rev. Lett. **103**, 153002 (2009).
[9] Xiaosong Zhu, Qingbin Zhang, Weiyi Hong, Pengfei Lan, and Peixiang Lu, Opt. Express **19**, 436 (2011).
[10] H. Akagi, T. Otobe, A. Staudte, A. Shiner, F. Turner, R. Dörner, D. M. Villeneuve, and P. B. Corkum, Science **325**, 1364 (2009).
[11] G. L. Kamta, A. D. Bandrauk, and P. B. Corkum, J. Phys. B **38**, L339 (2005).
[12] Xue-Bin Bian and A. D. Bandrauk, Phys. Rev. Lett. **105**, 093903 (2010).
[13] Y. Chen, Y. Li, S. Yang, and J. Liu, Phys. Rev. A **77**, 031402 (2008).
[14] Y. J. Chen, J. Liu, and Bambi Hu, Phys. Rev. A **79**, 033405 (2009).
[15] M. F. Ciappina, C. C. Chirilă, and M. Lein, Phys. Rev. A **75**, 043405 (2007).
[16] G. L. Kamta and A. D. Bandrauk, Phys. Rev. Lett. **94**, 203003 (2005).